

Jørgen Lauritzen Jensen

Quasi-non-linear fracture mechanics analysis of the splitting failure of single dowel joints loaded perpendicular to grain

Received: July 26, 2004 / Accepted: January 6, 2005

Abstract A quasi-non-linear fracture mechanics model based on beam on elastic foundation theory is applied for analysis of dowel joints with a single dowel loaded perpendicular to grain. The properties of the elastic foundation are chosen so that the perpendicular-to-grain tensile strength and fracture energy properties of the wood are correctly represented. It is shown that this particular choice of foundation stiffness makes a conventional maximum stress failure criterion lead to the same solution as the compliance method of fracture mechanics. Results of linear elastic fracture mechanics are obtained as a special case by assuming an infinitely large value of the foundation stiffness. Results of tests on so-called plate joints are compared with theoretical predictions, showing good agreement for variations in initial crack length as well as edge distance.

Key words Dowel joints · Perpendicular-to-grain load · Plate joint specimen · Quasi-non-linear fracture mechanics · Beam on elastic foundation

Introduction

Dowel-type fastener joints subjected to loading perpendicular to grain may fail in either a ductile manner, characterized by bending of the fastener and/or embedment of the fastener into the wood, or in a brittle manner characterized by splitting of the wood. The ductile failure modes are well understood and can be predicted with good accuracy by the European Yield Model, originally proposed by Johansen,¹ which now forms the basis of design of dowel-type fastener joints in major design codes. The brittle splitting failure mode is, however, not yet well understood. Although a few simple models suitable for implementation in design codes

have been proposed recently,^{2–7} none of those models have yet gained wide acceptance.

Plate joint specimens as shown in Fig. 1 have previously been used to derive relevant information on dowel-type fastener joints loaded perpendicular to grain.^{5,6,8} The model presented in this article considers a double symmetrical plate joint specimen with a single dowel, but may also be applied to joints in beams for which the edge distance, h_e , is small as compared with the total beam depth. The model is based on beam on elastic foundation (BEF) theory for a Timoshenko beam, and the foundation stiffness is associated with the fracture performance of the wood, i.e., perpendicular-to-grain tensile strength and mode I fracture energy.

A model based on the same ideas as the present model was previously reported⁹ considering joints with multiple dowels in a row parallel to grain. The previous model includes effects of edge distances, end distances, and dowel spacing. However, it does not address the effect of crack length, including dowel hole size, initial drying cracks, cracks occurring due to local compression damage in the wood beneath the dowel, etc. The effect of crack length is the main point of focus in the present article, which is limited to considering joints with a single dowel and with infinite end distances. Furthermore, the previous model⁹ was derived using conventional stress analysis and by introducing fracture mechanics through the constitutive relation of the foundation. In the present article, full derivations are given based on the compliance method of fracture mechanics and on the conventional stress approach, and it is shown that a certain choice of the foundation stiffness leads to the same predicted failure load with either approach.

Theory

The symmetrical half of the upper joint in Fig. 1 is modeled as a beam on elastic foundation as schematically shown in Fig. 2. A state, in which a crack of length $2a$ has developed, is considered. Let $w_0 = w(0)$ and $\theta_0 = \theta(0)$ denote the

J.L. Jensen (✉)
Institute of Wood Technology, Akita Prefectural University,
11-1 Kaiezaka, Noshiro 016-0876, Japan
Tel. +81-185-52-6985; Fax +81-185-52-6976
e-mail: jensen@iwt.akita-pu.ac.jp

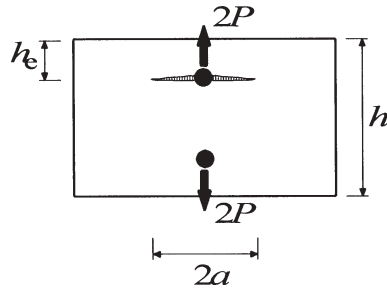


Fig. 1. Geometry of plate joint specimen

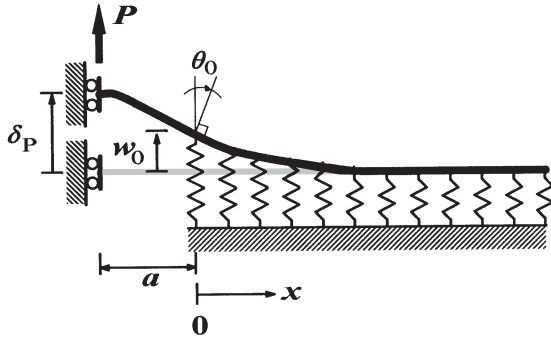


Fig. 2. Symmetrical half of plate joint modeled as beam on elastic foundation

displacement and rotation of the beam axis at $x = 0$, respectively, with positive directions as indicated in Fig. 2.

From the theory of a Timoshenko beam on elastic foundation^{10,11}

$$w_0 = \frac{1}{2EI\lambda^4}(\beta P_0 + \lambda^2 M_0), \quad \theta_0 = \frac{1}{EI\lambda^2} \left(\frac{1}{2} P_0 + \beta M_0 \right) \quad (1)$$

where

$$\lambda^4 = \frac{Kb}{4EI}, \quad \beta = \lambda \sqrt{1 + \frac{6EI}{5GA}} \lambda^2 \quad (2)$$

and where P_0 and M_0 are shear force and moment in the beam at $x = 0$, respectively, b is beam width, E is the modulus of elasticity (MOE) in the grain direction of the beam, G is the shear modulus of the beam, K is the stiffness of the elastic foundation (units: N/m^3), I is moment of inertia, and A is cross-sectional area of the beam (rectangular cross section is assumed).

For the structure shown in Fig. 2, P_0 and M_0 are found to be

$$P_0 = P, \quad M_0 = (1 - \kappa)Pa, \quad \kappa = \frac{\lambda^2 a^2 + 2\beta a + 1}{2\lambda^2 a^2 + 2\beta a} \quad (3)$$

Energy release rate failure criterion

The deflection at the loading point, δ_p , may be written

$$\delta_p = \delta_{pc} + \delta_{pw} + \delta_{p\theta} \quad (4)$$

where δ_{pc} is the contribution from the cantilever

$$\delta_{pc} = P \left(\frac{a^3}{EI} \left(\frac{1}{3} - \frac{1}{2}\kappa \right) + \frac{6a}{5GA} \right) \quad (5)$$

and δ_{pw} and $\delta_{p\theta}$ are the contributions from the beam on elastic foundation

$$\delta_{pw} = w_0 = \frac{P}{2EI\lambda^2} \left(\frac{\beta^2}{\lambda^2} + (1 - \kappa)a \right) \quad (6)$$

$$\delta_{p\theta} = a\theta_0 = \frac{P}{2EI\lambda^2} \left(1 + 2\beta(1 - \kappa)a \right) \quad (7)$$

The compliance, C , is given by $C = \delta_p/P$, and the increase in compliance due to an increase in crack length is found to be given by

$$\begin{aligned} \frac{dC}{da} = & \frac{1}{2(\lambda^2 a + \beta)^2} \left(\frac{1}{2EI} \left(\lambda^4 a^4 + 4 \frac{\lambda^4}{\beta} a^3 \right. \right. \\ & \left. \left. + 2(4\lambda^2 - \beta^2)a^2 + 4\beta a + 2 \frac{\beta^2}{\lambda^2} - 1 \right) \right. \\ & \left. + \frac{6}{5GA} \left(2 \frac{\lambda^6}{\beta} a^3 + 5\lambda^4 a^2 + 4\beta\lambda^2 a - \lambda^2 + 2\beta^2 \right) \right) \quad (8) \end{aligned}$$

For a linear elastic body loaded by a single load, P , the crack propagation energy release rate, \mathcal{G} , is given by¹²

$$\mathcal{G} = \frac{P^2 dC}{2b da} \quad (9)$$

A crack starts propagating when the energy release rate assumes a critical value, \mathcal{G}_c , i.e., the failure criterion is

$$\mathcal{G} = \mathcal{G}_c \quad (10)$$

Assuming static or quasi-static conditions and no energy dissipation outside the fracture region, the critical energy release rate is equal to the material property fracture energy, \mathcal{G}_f , i.e.,

$$\mathcal{G}_c = \mathcal{G}_f \quad (11)$$

From Eqs. 9–11 it follows

$$P_c = \sqrt{\frac{2b\mathcal{G}_f}{\frac{dC}{da}}} \quad (12)$$

Especially for $a \rightarrow 0$, Eqs. 8 and 12 lead to

$$P_{c0} = b \sqrt{\frac{h_c G \mathcal{G}_f}{3 \left(1 - \frac{\lambda^2}{2\beta^2} \right) \left(\frac{1}{\lambda^2 h^2} \frac{G}{E} + \frac{1}{5} \right)}} \quad (13)$$

Maximum stress failure criterion

The maximum tensile stress in the foundation occurs at $x = 0$ and is given by

$$\sigma_0 = Kw_0 \quad (14)$$

Failure is assumed to occur when the maximum tensile stress equals the perpendicular-to-grain tensile strength, i.e.,

$$\sigma_0 = f_t \quad (15)$$

From Eqs. 1, 3, 14, and 15 it follows that

$$P_c = \frac{1}{2}bf_t \frac{1}{\beta + (1 - \kappa)\lambda^2 a} \quad (16)$$

Especially for $a \rightarrow 0$, Eq. 16 leads to

$$P_{c0} = bf_t \frac{\beta}{2\beta^2 - \lambda^2} \quad (17)$$

Foundation properties

The deformation of the foundation is, in general, assumed to be composed of a contribution from a special fracture layer (with no physical thickness) modeling the fracture damage and a contribution from the perpendicular-to-grain elastic strains in the wood as indicated in Fig. 3.

The damage and fracture performance of wood is in general nonlinear, but is in the present analysis represented by a linear response that is equivalent in terms of peak stress, f_t , and fracture energy dissipation, G_f . Because the special fracture layer has no physical perpendicular-to-grain dimension, strain is not defined and the perpendicular-to-grain stress, σ , is used as constitutive relation as a function of the perpendicular-to-grain deformation, δ_f .

From Fig. 4, it follows that the stiffness of the fracture layer, K_f , is given by

$$K_f = \frac{f_t^2}{2G_f} \quad (18)$$

The elastic perpendicular-to-grain strain, ε_s , in the wood is given by Hook's law, and the deformation, δ_s , and stiffness, K_s , of the part of the specimen between the beam axis and horizontal line of symmetry is given by

$$\delta_s = \frac{1}{2}(h - h_e)\varepsilon_s = \frac{h - h_e}{2E_y}\sigma \Rightarrow K_s = \frac{2E_y}{h - h_e} \quad (19)$$

The slice of the foundation shown in Fig. 3 is assumed to be in a state of uniaxial stress, and the total stiffness of the foundation is thus given by

$$K = \frac{K_f K_s}{K_f + K_s} \quad (20)$$

In previous applications of beam on elastic foundation theory to mode I fracture problems,^{11,13,14} the special frac-

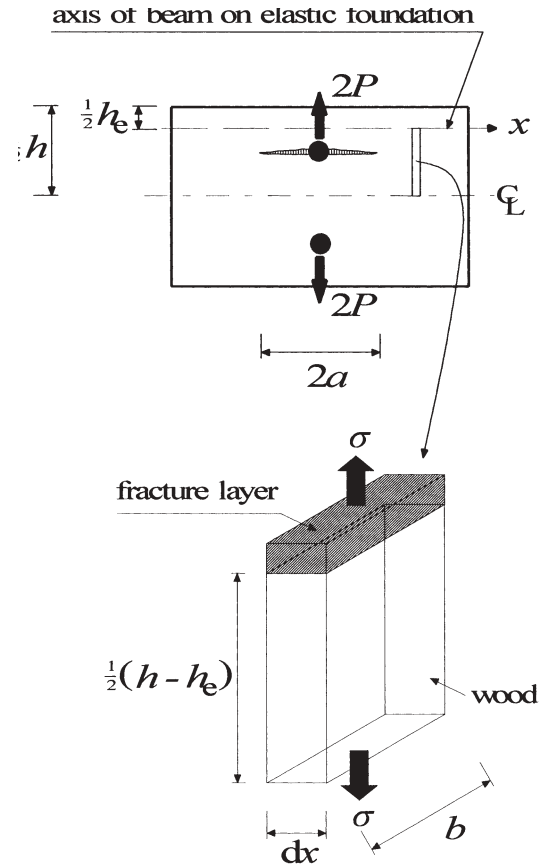


Fig. 3. Contributions to foundation stiffness

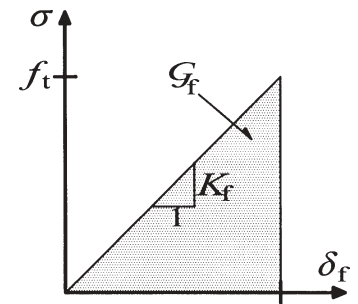


Fig. 4. Constitutive relation of fracture layer

ture layer as considered in the present article was omitted, and the deformations of the foundation have been attributed solely to the elastic perpendicular-to-grain strains. If disregarding the elastic perpendicular-to-grain strains, i.e., $K_s \rightarrow \infty$, then

$$K = \frac{f_t^2}{2G_f} \quad (21)$$

Using the stress approach as given by Eq. 16 or 17 together with Eq. 21 is a complete analogy to the fracture mechanics application of the Volkersen model to analysis of mode II failure in lap joints.¹⁵ The analysis has been termed

quasi-non-linear fracture mechanics because the material responses are assumed to be linear as in linear elastic fracture mechanics (LEFM). However, at the same time, the tensile strength is assigned a finite value, not an infinite value as in LEFM, and, while it is a characteristic of LEFM that the failure load is proportional to the square root of the fracture energy, this is not a characteristic of the quasi-non-linear fracture mechanics model. Equation 21 ensures that the fracture mechanics and stress approaches lead to the same failure load. In general, when using BEF theory it is significantly easier to derive simple solutions by means of the stress approach than by the fracture mechanics approach. Equation 21 makes Eqs. 13 and 17 lead to the same solution as previously derived for glued-in rods subjected to pure shear^{9,16} and for the splitting strength of dowel joints loaded perpendicular to grain.¹⁶ This solution may be written (note that the total failure load of the plate joint specimen according to Fig. 1 is $2P_{c0}$).

$$P_{c0} = \gamma P_{LEFM}$$

$$P_{LEFM} = bC_1\sqrt{h_c}, \quad \gamma = \frac{\sqrt{2\xi + 1}}{\xi + 1} \quad (22)$$

$$\xi = \frac{C_1}{f_t} \sqrt{10 \frac{G}{E} \frac{1}{h_c}}, \quad C_1 = \sqrt{\frac{5}{3} G G_f}$$

For f_t or $E \rightarrow \infty$, the failure load according to Eq. 22 becomes $2P_{c0} = 2b(5GG_f h_c/3)^{1/2}$. This is the same solution as previously obtained by using a fracture energy balance equation and a chosen displacement field, which considers only shear deformations,^{5,6} if in the latter solution the shear area $A_s = 5bh_c/6$ is used instead of the full cross sectional area $A = bh_c$, and the same solution as predicted for $h_c/h \rightarrow 0$ by another previous LEFM solution.^{2,7,8}

Figure 5 shows an example of the influence of crack length, a , on the failure load according to Eqs. 8 and 12 or Eq. 16. Equation 21 has been assumed, and the material and geometrical properties used are: $h_c = 40$ mm, $b = 25$ mm, $E = 5670$ MPa, $G = 315$ MPa, $f_t = 3.5$ MPa, $G_f = 0.20$ N/mm.

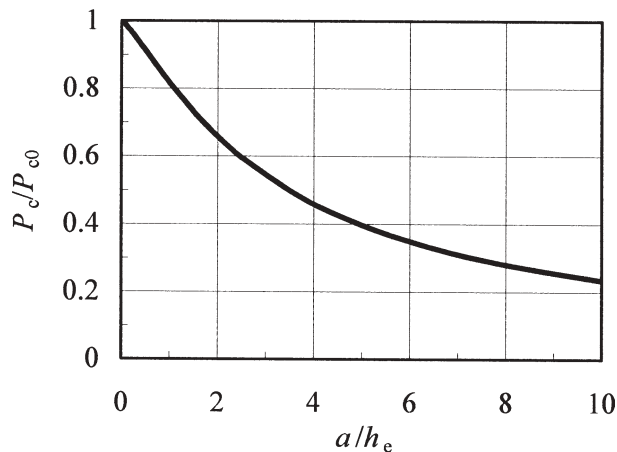


Fig. 5. Influence of crack length on the failure load

Figure 6 shows $\gamma = P_{c0}/P_{LEFM}$ as given by Eq. 22 as a function of the perpendicular-to-grain tensile strength. The same b , E , G , and G_f as used in Fig. 5 apply to Fig. 6. The sensitivity to variations in f_t is similar for finite values of the initial crack length (Eqs. 16 and 21).

Experimental

Three test series were conducted on plate joint specimens. Series 1 was conducted in order to evaluate the influence of the initial crack length. Series 2 was conducted to evaluate the influence of the edge distance. Series 3 was conducted to evaluate the influence of elastic perpendicular-to-grain strains.

Methods and materials

All specimens were made of glulam of Japanese cedar (*Cryptomeria japonica*). The MOE in the grain direction was determined by measuring the longitudinal vibration frequency of the glulam beams, from which the specimens were cut. All tests were displacement controlled and time to failure was 2–3 min. All tests were conducted using a 14-mm dowel in a 15-mm hole. Specimens were not especially selected to avoid knots or other defects.

Series 1 was conducted to evaluate the influence of the initial crack length, a . All specimens had dimensions of $b = 25$ mm, $h = 200$ mm, $h_c = 40$ mm, and $L = 500$ mm. Ratios $a/h_c = 0, 0.5, 1$, and 2 were tested. The moisture content (MC) was 10.5%, density was 370 kg/m³ at 10.5% MC, and the MOE was 5670 MPa. Twenty specimens were tested for $a/h_c = 0$, and ten specimens were tested for other a/h_c ratios. The cracks were cut with a small band saw resulting in a crack width of 1 mm. The reported crack length is the length of the cut crack, i.e., from crack tip to the dowel hole periphery. Tensile strength perpendicular to grain was

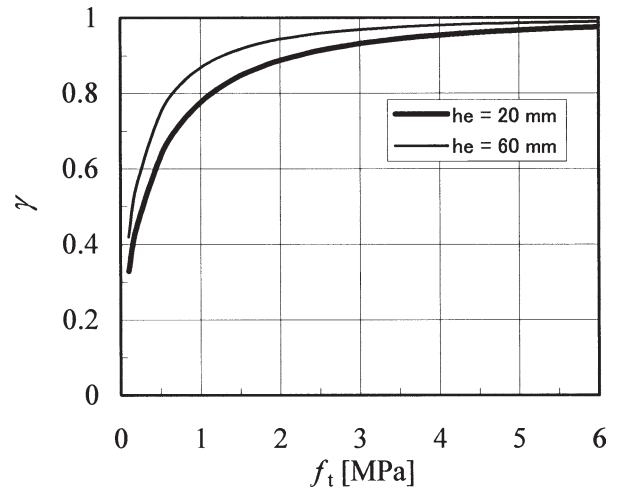


Fig. 6. Normalized failure load as a function of perpendicular-to-grain tensile strength for zero crack length

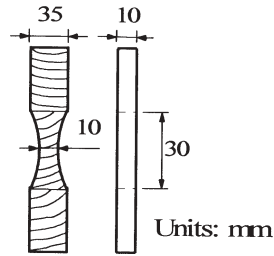


Fig. 7. Test specimen for determination of perpendicular-to-grain tensile strength

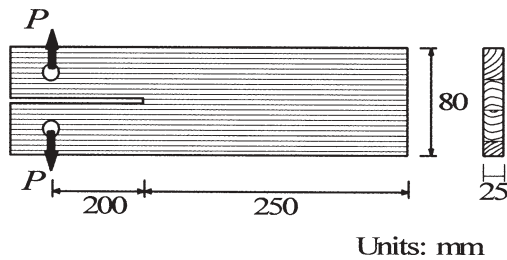


Fig. 8. Double cantilever beam specimen for determination of fracture energy

determined using specimens as shown in Fig. 7. Twenty-four specimens were tested. Fracture energy was determined using DCB specimens as shown in Fig. 8, and using Eq. 23 with $b = 25$ mm, $h = 40$ mm, $a = 200$ mm, and $G = E/18$.

$$G_t = \frac{12P_c^2}{Eb^2h} \left(\frac{a}{h} + \sqrt{\frac{1}{10} \frac{E}{G}} \right)^2 \quad (23)$$

Series 2 was conducted to evaluate the influence of edge distance, h_e . Specimens were cut from the same beams as the specimens used in series 1. In series 2, no initial cracks were cut, i.e., $a = 0$. All other conditions were the same as for series 1. Twenty specimens were tested for $h_e = 40$ mm (from series 1), and ten specimens were tested for $h_e = 20$ mm and for $h_e = 60$ mm.

Series 3 was conducted to evaluate the influence of the elastic strains in the wood. All specimens had dimensions of $b = 40$ mm, $h_e = 56$ mm, $L = 500$ mm, and no initial cracks were cut, i.e., $a = 0$. Two values of specimen depth were tested: $h = 800$ mm (seven specimens) and $h = 200$ mm (ten specimens). The MC was 12%, and the MOE was 11 363 MPa.

Results and discussion

Series 1

The tension tests gave a value of the perpendicular-to-grain tensile strength, f_t , of 3.5 ± 1.1 MPa (mean value \pm standard deviation), and the fracture energy tests gave a fracture energy, G_t of 0.20 ± 0.06 N/mm. Figure 9 shows the normal-

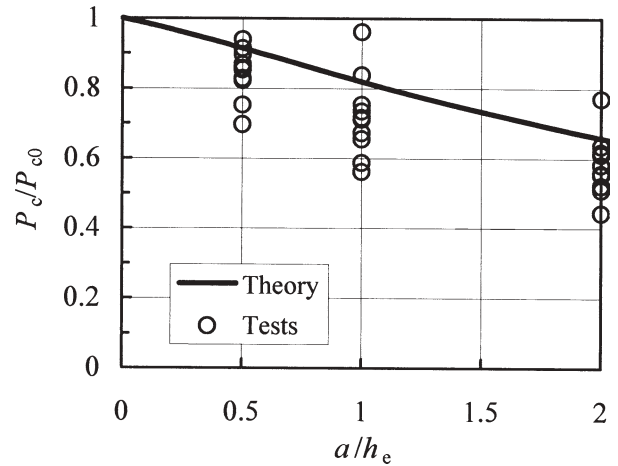


Fig. 9. Calculated and tested failure loads as a function of the initial crack length

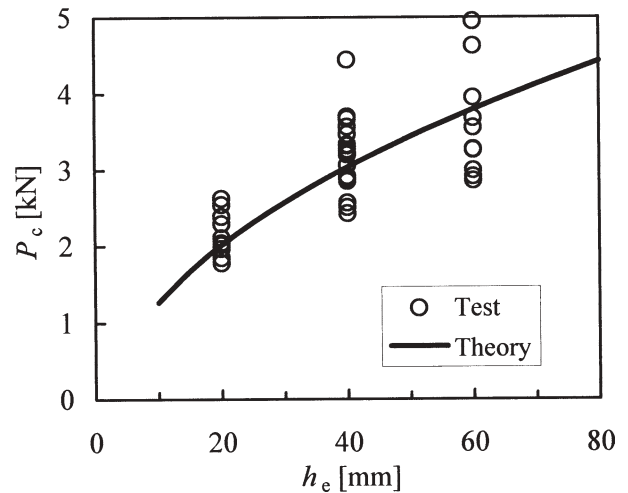


Fig. 10. Calculated and tested failure loads as a function of the edge distance

ized failure load, P_c/P_{c0} , as a function of the normalized initial crack length, a/h_e . P_{c0} for the tested values is taken as the mean value of failure load for $a = 0$ mm ($P_{c0} = 3.15$ kN). Note that a here denotes the length of the (half) crack cut by saw, i.e., the dowel hole is not counted as a part of the initial crack. If the dowel hole is counted as part of the initial crack, the tested a/h_e values thus become 0.69, 1.19, and 2.19 instead of the values 0.5, 1.0, and 2.0, respectively, as given in Fig. 9; this leads to even better agreement between theory and experiment than indicated in Fig. 9. The theoretical failure loads have been calculated using Eqs. 16 and 17 with the foundation stiffness as given by Eq. 21.

Series 2

Figure 10 shows the failure load, P_c , as a function of the edge distance, h_e . The theoretical values have been calcu-

lated using Eqs. 16 and 21 with $f_t = 3.5$ MPa and $G_f = 0.20$ N/mm (as determined by means of tensile and DCB specimen test). The maximum embedment at failure observed in series 1 and 2 was about 2 mm.

The perpendicular-to-grain tensile strength of wood depends heavily on the volume subjected to maximum stress, and an appropriate volume (or cross-sectional area) of the tensile strength specimen is not obvious. It has previously been suggested to use the plate joint specimen as a standard test specimen for deriving a so-called fracture parameter,⁸ $C_1 = (5G_f/3)^{1/2}$. Similarly, the foundation stiffness or the perpendicular-to-grain tensile strength may, in principle, be derived from standard plate joint tests if the fracture energy is known.

From Eqs. 17 and 21 it follows

$$K = \frac{25}{3} \frac{G^2}{Eh_e} \left(\frac{\varepsilon}{1 - \varepsilon + \sqrt{1 - \varepsilon}} \right)^2, \quad \varepsilon = \frac{3}{5} \frac{P_c^2}{b^2 G_f h_e} \quad (24)$$

and

$$f_t = \sqrt{2KG_f} \quad (25)$$

As seen from Fig. 6, the predicted failure load asymptotically approaches an upper limit for $f_t \rightarrow \infty$ (and thus $K \rightarrow \infty$). If the predicted failure load is based on the mean value of G_f obtained from DCB specimen tests, some individual failure loads obtained by plate joint tests may exceed the predicted upper limit due to the fact that the fracture energy of the individual specimen may be considerably higher (typically caused by knots) than the mean value. This effect leads to $\varepsilon > 1$ and causes numerical problems in Eq. 24. Equations 24 and 25 should thus not be used on individual plate joint test results, but only on mean values for which numerical problems are less likely to occur.

Using $G_f = 0.20$ N/mm as obtained from the DCB specimen tests, Eqs. 24 and 25 lead to $f_t = 3.5$ MPa for $h_e = 20$ mm, $f_t = 3.9$ MPa for $h_e = 40$ mm, and $f_t = 1.4$ MPa for $h_e = 60$ mm. Figure 6 shows that the quasi-non-linear fracture mechanics solution for the plate joint is relatively insensitive to variations in f_t in the range relevant for glulam. For example, the increase in failure load for $h_e = 20$ mm when increasing f_t from 1.4 MPa to 3.5 MPa is only about 13%. Relatively small variations in failure loads may thus cause large variations in the perpendicular-to-grain tensile strengths determined by means of Eqs. 24 and 25, which explains the significantly lower f_t value obtained for $h_e = 60$ mm.

Series 3

P_{c200} and P_{c800} denote the failure loads of specimens with $h = 200$ mm and $h = 800$ mm, respectively (all other properties being the same). The tests gave the following mean values \pm standard deviation: $P_{c200} = 6.16 \pm 0.37$ kN and $P_{c800} = 6.71 \pm 0.30$ kN. *F*-test and Student's *t*-test indicate that the two specimens can be assumed to have same variation, but different mean values of the failure load. No excessive embedment of the dowel was observed.

Table 1. Calculated failure load ratios P_{c200}/P_{c800}

Assumption	Equation 13	Equation 17
$K = f_t^2/2G_f$	1.00	1.00
$K = 2E_f/(h - h_e)$	1.19	0.52

Table 1 shows the calculated failure load ratios, P_{c200}/P_{c800} , given using Eq. 13 (fracture mechanics approach for $a = 0$) and Eq. 17 (stress approach for $a = 0$) assuming either $K = f_t^2/2G_f$ (i.e., disregarding the elastic strains) or $K = 2E_f/(h - h_e)$ (i.e., disregarding the fracture layer). Note that the calculated failure load ratios are all independent of f_t and G_f . The value of P_{c200}/P_{c800} found by testing is 0.92. Although the test results of series 3 are too sparse to make any firm conclusion, a value of the foundation stiffness independent of h as given by Eq. 21 ($K = f_t^2/2G_f$) seems to be the most appropriate choice.

Conclusions

A quasi-non-linear fracture mechanics model for analysis of dowel-type fastener joints with a single fastener subjected to perpendicular-to-grain loading was presented. The model is based on Timoshenko beam on elastic foundation theory, which includes shear deformations, and it takes into account the crack length. The analysis includes a fracture mechanics approach based on the compliance method and a conventional stress approach. The properties of the linear foundation (fracture layer) are chosen so that the perpendicular-to-grain tensile strength and fracture energy properties of the wood are correctly represented. This particular choice of foundation stiffness was shown to unify the stress and compliance approaches. Some previous LEFM models^{2,5,7} were shown to appear as special cases of the quasi-non-linear fracture mechanics model. The quasi-non-linear fracture mechanics model was found to be able to predict the influence of edge distance and initial crack length in good agreement with test results.

Quasi-non-linear fracture mechanics models based on BEF theory require the perpendicular-to-grain tensile strength, f_t , as an input, but because f_t is highly volume dependent, direct determination by tension tests requires a method for estimation of a proper volume (or cross section) of the test specimen. The plate joint specimen has previously been proposed as a standard test specimen for deriving relevant fracture properties for use in LEFM models.^{5,6,8} However, the plate joint specimen seems to be too insensitive to variations in the perpendicular-to-grain tensile strength. Standard test specimens more sensitive to variations in f_t than the plate joint specimen should therefore be sought for determination of the perpendicular-to-grain tensile strength.

References

1. Johansen KW (1941) Forsøg med træforbindelser. Bygningsstatistiske Meddelelser, årgang XII
2. Van der Put TACM, Leijten AJM (2000) Evaluation of perpendicular-to-grain failure of beams caused by concentrated loads of joints. In: Proceedings of the International Council for Research and Innovation in Building and Construction, CIB-W18 Meeting Thirty-Three, Delft, The Netherlands, paper No. 33-7-7
3. Leijten AJM, Jorissen AJM (2001) Splitting strength of beam loaded by connections perpendicular to grain, model validation. In: Proceedings of the International Council for Research and Innovation in Building and Construction, CIB-W18 Meeting Thirty-Four, Venice, Italy, paper No. 34-7-1
4. Leijten AJM (2002) Splitting strength of beams loaded by connections, model comparison. In: Proceedings of the International Council for Research and Innovation in Building and Construction, CIB-W18 Meeting Thirty-Five, Kyoto, Japan, paper No. 35-7-7
5. Gustafsson PJ, Larsen HJ (2001) Dowel joints loaded perpendicular to grain. In: Aicher S, Reinhardt HW (eds) Joints in timber structures. Proceedings of the International RILEM Symposium, Stuttgart, Germany, pp 577–586
6. Larsen HJ, Gustafsson PJ (2001) Dowel joints loaded perpendicular to grain. In: Proceedings of the International Council for Research and Innovation in Building and Construction, CIB-W18 Meeting Thirty-Four, Venice, Italy, paper No. 34-7-3
7. Jensen JL (2003) Splitting strength of beams loaded by connections. In: Proceedings of the International Council for Research and Innovation in Building and Construction, CIB-W18 Meeting Thirty-Six, Colorado, USA, paper No. 36-7-8
8. Yasumura M (2002) Determination of fracture parameter for dowel-type joints loaded perpendicular to wooden grain and its application. In: Proceedings of the International Council for Research and Innovation in Building and Construction, CIB-W18 Meeting Thirty-Five, Kyoto, Japan, paper No. 35-7-9
9. Jensen JL, Gustafsson PJ, Larsen HJ (2003) A tensile fracture model for joints with rods or dowels loaded perpendicular to grain. In: Proceedings of the International Council for Research and Innovation in Building and Construction, CIB-W18 Meeting Thirty-Six, Colorado, USA, paper No. 36-7-9
10. Pilkey WD (1994) Formulas for stress, strain, and structural matrices. Wiley, New York
11. Jorissen AJM (1998) Double shear timber connections with dowel-type fasteners. Delft University Press, Delft, The Netherlands
12. Hellan K (1984) Introduction to fracture mechanics. McGraw-Hill, New York, pp 49–72
13. Wernersson H (1994) Fracture characterization of wood adhesive joints. Report TVSM-1006, Lund University, Lund Institute of Technology, Division of Structural Mechanics, Sweden
14. Komatsu K, Sasaki H, Maku T (1976) Strain energy release rate of double cantilever beam specimen with finite thickness of adhesive layer. Wood Res 59:80–92
15. Gustafsson PJ (1987) Analysis of generalized Volkersen-joints in terms of non-linear fracture mechanics. In: Verchery G, Cardon AH (eds) Mechanical behaviour of adhesive joints. Pluralis, Paris, pp 323–338
16. Jensen JL, Gustafsson PJ (2004) Shear strength of beam splice joints with glued-in rods. J Wood Sci 50:123–129